Asian Journal of Conservation Biology, December 2023. Vol. 12 No. 2, pp. 179–188 AJCB: FP0221/83427
ISSN 2278-7666 ©TCRP Foundation 2023 https://doi.org/10.53562/ajcb.83427

Research Article

A new species of the genus *Cnemaspis* Strauch, 1887 (Squamata: Gekkonidae) from the higher elevations of Tamil Nadu, India

Amit Sayyed[1*], Samson Kirubakaran[1], Rahul Khot[2], Thanigaivel A[1, 3], Satheeshkumar M[1], Ayaan Sayyed[1], Masum Sayyed[1], Jayaditya Purkayastha[1,4], Shubhankar Deshpande[1, 5] and Shauri Sulakhe[1, 5]

[1] *Wildlife Protection and Research Society (WLPRS), Satara, Maharashtra, India*
[2] *Bombay Natural History Society, Mumbai, Maharashtra, India*
[3] *Ashoka Trust for Research in Ecology and the Environment (ATREE), Bengaluru, Karnataka, India*
[4] *Help Earth, 16, RNC Path, Lachitnagar, Guwahati 781007, Assam, India*
[5] *InSearch Environmental Solutions (IES), Flat No:1, Omkar apartment, Kothrud, Pune, India*

(Received: September 16, 2023 ; Revised: November 01, 2023; Accepted: November 04, 2023)

ABSTRACT

In this study, we present the description of a previously undocumented species of *Cnemaspis* found in the region of Tamil Nadu, India. Molecular analysis of the species reveals its placement within the *Cnemaspis beddomei* Theobald, 1876 clade, with a range of genetic divergence on the ND2 gene, spanning from 9.5% to 30.2% in comparison to its congeners. Although bearing a resemblance to the well-known *Cnemaspis ornata* Beddome, 1870, the new species exhibits a distinct set of non-overlapping morphological characteristics that set it apart. These findings are supported by molecular data, solidifying the distinction between the newly described species and its close relatives.

Key words: *Cnemaspis beddomei* clade, phylogeny, systematics, taxonomy, ND2.

INTRODUCTION

The Western Ghats escarpment is a part of India and has the oldest region of differentiation of flora and fauna that supports large evolutionary radiations (Mani, 1974; Biju *et al.* 2014; Vijaykumar *et al.* 2016; Chaitanya *et al.* 2019; Loria & Prendini, 2020). Several taxa are restricted to the higher elevations of the Western Ghats, thus being micro-endemic to that region (Vijaykumar *et al.* 2016; Pal *et al.* 2021).

The genus *Cnemaspis* Strauch, 1887 is known for its high species diversity in peninsular India showing distinct micro-endemism (Sayyed *et al.* 2019; Pal *et al.* 2021; Agarwal *et al.* 2022; Sayyed *et al.* 2023 a, b). Currently, the South Asian members of the genus consist of ten clades (Pal *et al.* 2021) and a total of 85 described species in India (Utez *et al.* 2023). Amongst these ten clades, *Cnemaspis beddomei* Theobald, 1876 clade is restricted to the southern Western Ghats (SWG) of India (Pal *et al.* 2021). The recent surveys and findings of new species in the Western Ghats of India have contributed to an increased count of species within the *C. beddomei* clade (Sayyed *et al.* 2019; Pal *et al.* 2021) and further, the discordance between phylogeny and geography in the *C. beddomei* clade was highlighted in this publication.

In this paper, we describe a new species of *Cnemaspis* within the *C. beddomei* clade from Kottamalai estate, Settur, Rajapalayam, Virudhunagar district, Tamil Nadu which shows a close affinity with *Cnemaspis ornata* species with the lectotype and para-lectotype series of *C. ornata* deposited in the The Natural History Museum, London, UK (NHMUK (formerly BMNH)) based (Sayyed *et al*. 2019). Furthermore, we also give detailed comparisons of the new species with the congeners based on morphological and genetic data.

MATERIALS AND METHODS

Sampling

Field surveys were conducted in both day and night time, in parts of Tamil Nadu, India. Type specimens were collected by hand from rock boulders, photographed in life, and then euthanized using halothane following the guidelines by Leary *et al.* (2013). Thigh tissues of specimens (BNHS 2922 and BNHS 2924) were collected and used for further molecular work. Subsequently, specimens were fixed in 4% formaldehyde for ~24 hours, washed in water, and transferred to 70% ethanol for long-term storage. Scalation and other morphological characters were recorded using a Lensel stereo microscope. The materials referred to in this study are deposited in the collection of the Bombay Natural History Society (BNHS), Mumbai, India.

Morphological study

Morphological data (to the nearest 0.01 mm) was recorded as Snout-vent length (SVL), distance from tip of snout to anterior margin of vent; axilla-groin length

[*]*Corresponding Author's E-mail: amitsayyedsatara@gmail.com*

(AG), distance from axilla to groin; trunk width (TW),maximum width of the body; eye diameter (ED), horizontal diameter of the orbit; eye-to-nares (EN), distance between anterior point of the orbit to the posterior part of the nostril; snout length (ES), distance from anterior margin of the orbit to the tip of the snout; eye-to-ear (ET), distance from posterior margin of the orbit to the anterior margin of the ear opening; internarial distance (IN), least distance between the inner margins of the nostrils; ear opening diameter (EOD), horizontal distance from the anterior to posterior margin of the ear opening; head length (HL), distance from tip of snout to posterior edge of mandible; head width (HW), maximum width of the head; head depth (HD), maximum depth of the head; interorbital distance (IO), shortest distance between the superciliary scale rows; upper arm length (UAL), distance from axilla to elbow, lower arm length (FAL), distance from elbow to wrist; Finger length (FL), distance from the tip of the finger to the nearest fork; femur length (FEL), distance from groin to the knee; tibia length (TBL), distance from knee to heel toe length; (TOL), distance from tip of 1st toe to the nearest fork; tail length (TL), distance between posterior margin of vent to the tip of the tail.

Meristic data recorded for all specimens included number of supralabials (SupL) and infralabials (InfL) on left (L) and right (R) sides; number of supraciliaries (SuS); number of interorbital scales (InO); number of scales between eye to tympanum (BeT), from posterior-most point of the orbit to anterior-most point of the tympanum; number of the postnasal (PoN),all scales posterior to the naris; number of postmentals (PoM); number of posterior postmentals (PoP), scales that are surrounded by the posterior-postmentals and between infralabials; number of supranasal (SuN), excluding the smaller scales between the larger supranasals; number of canthal scales (CaS), number of scales from posterior-most point of naris to anterior most point of the orbit; number of mid-dorsal scales (MbS), from the centre of mid-dorsal row diagonally towards the ventral scales; dorsal tubercle rows (DtR), longitudinal rows of enlarged tubercles; number of mid-ventral scales (MvS), from the first scale posterior to the mental to last scale anterior to the vent; number of mid-body scales (BlS), across the ventral between the lowest rows of dorsal scales; precloacal pores (PPores), the number of precloacal pores; lamellae under digits of manus (MLam) and pes (PLam) on right (R) side, counted from first proximal enlarged scansor greater than twice width of the largest palm scale, to distalmost lamella at tip of digits; lamellae under fourth digit of pes (LampIV). Morphometric data are given as % of SVL. Morphological data were taken using a Mitutoyo 500, (to the nearest 0.1 mm). For the geographical coordinates and altitude readings, we used a Kestrel 4500 receiver.

Molecular analysis

DNA extraction, amplification, and sequencing: DNA extraction, amplification and sequencing protocols for ND2 (Sayyed *et al.* 2023a, b) were followed. The genomic DNA of *Cnemaspis* specimens (was extracted from muscle tissue (thigh tissue) samples that were preserved in 100% ethanol. The DNA extraction was carried out using a DNeasy (QiagenTM) blood and tissue kit following the manufacturer's instructions. Partial sequences of the mitochondrial NADH dehydrogenase 2 (ND2) gene of the new species were amplified. The amplification of the ND2 gene was carried out in three steps of polymerase chain reaction (PCR) using primers MetF1 (Forward) and H5934 (Reverse) (Macey *et al.* 1997). The fragments were amplified with the following conditions: 95°C – 3 min, 1 cycle, 95°C – 30 sec, 56–58°C – 30 sec, 72°C – 45 sec, 35 Cycles, 72°C – 7 min.

Sequence alignments: The ND2 sequences were cleaned manually with MEGA v.7 (Kumar *et al.* 2016) using chromatograms visualised in Chromas v.2.6.5 (Technelysium Pty. Ltd.). Comparative ND2 and 16S sequences comprising members of the *Cnemaspis* were downloaded from GenBank following (Pal *et al.* 2021; Agarwal *et al.* 2022; Narayanan & Aravind 2022; Narayanan *et al.* 2023; Sayyed *et al.* 2023) and newly generated sequences were deposited in the GenBank® (Benson *et al.* 2017) under accession numbers as per Appendix 1. The sequences were aligned using MUSCLE (Edgar 2004) in MEGA v.7 (Tamura & Nei, 1993, Kumar *et al.* 2016) with default parameter settings. The final ND2+16S rRNA alignment contained cumulatively 19 sequences.

Molecular phylogenetics analysis: Maximum Likelihood (ML) and Bayesian Inference (BI) methods of phylogenetic analyses were implemented. The ND2 region was partitioned per codon position, whereas the non-coding 16S rRNA region was not partitioned. The model search for the ML analysis was performed with a greedy search algorithm (Schwarz, 1978) and models were selected using the Akaike Information Criterion (AIC). ML analysis was performed using the web implementation of IQ-tree (Nguyen *et al.* 2015) under the following models of sequence evolution: GTR+F+I+G4 for partition 1 , TVM+F+I+G4 for partition 2, TIM3+F+G4 for partition 3 of ND2 and GTR+F+I+G4 for partition 4 for 16S rRNA. The model of sequence evolution was determined using ModelFinder (Kalyaanamoorthy *et al.* 2017) on the IQ-tree web platform, and branch support was tested using 1000 non-parametric rapid ultrafast bootstrap pseudo-replicates (Minh *et al.* 2020). Bayesian trees were generated using MrBayes v.3.2.6 (Ronquist *et al.* 2012). Model search for the BI analysis was performed with a greedy search algorithm (Schwarz, 1978) and models were selected using the Bayesian Information criterion (BIC). The best substitution model for BI phylogenetic analysis was determined using PartitionFinder v.1.1.1 (Lanfear *et al.* 2012). The models of sequence evolution were as follows: GTR+I+G for codon partition 1, 2 and 4 and GTR+G for codon partition 3. For the BI analysis, two simultaneous, independent analyses were run starting from different random trees. Three heated and one cold chain were used in the analysis. The analysis was run for 10 million generations and Markov chains were sampled every 200 generations. At the end of the run, we tested the convergence of the two MCMC runs by checking the standard deviation of split frequencies, which was less than 0.001, and by checking the trace plots using Tracer v.1.7 (Rambaut *et al.* 2018). The Effective Sample Size (ESS) values for all the parameters were above 200, further indicating convergence. A total of 25% of trees were discarded as burn-in. The tree representing the best evolutionary hypothesis was selected using a 50% majority consensus rule. The generated trees only show the projection of *C. beddomei* clades. Genetic divergence (*p*-distance). The *p*-distances were

calculated for the ND2 gene in MEGA v.7. The substitution type was set as nucleotide, the model was kept as p-distance and the substitutions were included as d: Transitions + Transversions. Uniform rates were kept for analysis. Missing data were pairwise deleted and the site cutoff was set as 95%. The *p*-distances are mentioned in Table 1.

Etymology. Specific epithet is a patronym in honour of Prof. Rashid Sayyed, father of the first author.

Suggested Common Name: Rashid's dwarf gecko

Table 1. Pairwise uncorrected ND2 sequence divergence between new species, and other members of the *Cnemaspis beddomei* clade. *C. nairi* and *C. rubraoculus* are not included in the table due to the unavailability of the sequences for the ND2 gene.

No.	Species	1	2	3	4	5	6	7	8	9	10	11	12	13	14	15	16
1	OR714921 *Cnemaspis rashidi* **sp. nov.**																
2	OR714922 *Cnemaspis rashidi* **sp. nov.**	0.000															
3	BNHS 2915 *Cnemaspis sp.*	0.290	0.289														
4	BNHS 2916 *Cnemaspis sp.*	0.290	0.289	0.000													
5	MZ701818 *Cnemaspis galaxia*	0.302	0.301	0.148	0.148												
6	OR714926 *Cnemaspis aaronbaueri*	0.287	0.282	0.159	0.159	0.205											
7	OR714927 *Cnemaspis aaronbaueri*	0.297	0.293	0.163	0.163	0.205	0.003										
8	ON494554 *Cnemaspis azhagu*	0.300	0.295	0.157	0.157	0.136	0.101	0.106									
9	MZ701816 *Cnemaspis regalis*	0.264	0.257	0.157	0.157	-	0.117	0.122	0.076								
10	MZ701809 *Cnemaspis ornata*	0.097	0.095	0.275	0.275	0.290	0.266	0.281	0.276	0.255							
11	MZ701808 *Cnemaspis nigriventris*	0.159	0.154	0.316	0.316	0.320	0.299	0.299	0.309	0.000	0.185						
12	MZ701805 *Cnemaspis anamudi-ensis*	0.264	0.264	0.286	0.286	0.339	0.292	0.303	0.278	0.266	0.263	0.255					
13	MZ701807 *Cnemaspis nimbus*	0.278	0.262	0.321	0.321	0.355	0.305	0.305	0.304	0.238	0.273	0.269	0.110				
14	MZ701813 *Cnemaspis wallaceii*	0.286	0.271	0.305	0.305	0.340	0.314	0.314	0.261	0.217	0.276	0.287	0.127	0.143			
15	MZ701814 *Cnemaspis beddomei*	0.283	0.283	0.283	0.283	0.333	0.285	0.285	0.256	0.222	0.305	0.260	0.232	0.220	0.213		
16	MZ701825. *Cnemaspis* cf. *macu-licollis*	0.274	0.262	0.277	0.277	0.332	0.302	0.311	0.294	0.287	0.293	0.316	0.261	0.270	0.267	0.186	
17	MZ701806 *Cnemaspis smaug*	0.290	0.283	0.301	0.301	0.322	0.316	0.316	0.300	-	0.300	0.290	0.257	0.257	0.239	0.202	0.184

Molecular Analysis (Fig. 6)

Phylogenetic relationships.

The tree topology recovered is in agreement with the trees generated by Pal *et al.* (2021). The ML and BI analyses based on the concatenated dataset of ND2+16S rRNA genes showed *C. rashidi* **sp. nov.** to be a member of *C. beddomei* clade. *Cnemaspis rashidi* **sp. nov.** was recovered as a sister to *C. ornata* in both ML and BI analyses with a high bootstrap (bp) support value of 100 and posterior probability (pp) value of 1. *Cnemaspis rashidi* **sp. nov.** *was* recovered nearest to *C. ornata* and can be separated with a genetic divergence of 9.5–9.7%.

Systematics

Cnemaspis rashidi **sp. nov.,**
Figs 1, 2, 3, 4. Table 2, 3

urn:lsid:zoobank.org:act:990D2662-AA75-4CAF-AE60-5E065283FDC6

Holotype. Adult male, BNHS 2921 (47.50 mm SVL), collected on the rock boulder (9.500463N, 77.406013E; ca. 1245 m asl.) in Kottamalai estate, Settur, Rajapalayam, Viridhunagar district, Tamil Nadu, India; collected by Amit Sayyed and Samson Kirubakaran on 05 May 2015.

Paratypes (n=3). Adult female BNHS 2922 (47.29 mm SVL), adult male BNHS 2923 (49.93 mm SVL), sub-adult male BNHS 2924 (42.34 mm SVL), locality and collection data same as holotype.

Diagnosis.

A medium sized, *Cnemaspis* with adult SVL<50 mm (*n*=4); dorsal scales heterogeneous; circular granular scales intermixed with enlarged, fairly regularly arranged, strongly keeled, pointed, conical tubercles; scales on flanks small, granular, smooth, slightly raised, conical and spine-like tubercles absent on either side of the lower flanks; 7–8 supralabials; 7 infralabials; 10–11 longitudinal rows of enlarged tubercles on dorsal body; mid-dorsal scales 73–75; scales on snout and canthus rostralis large, round, juxtaposed, un-keeled; scales on nape, ventral surface of neck, occipital and temporal region granular, small, round, un-keeled; rostral groove present; mental enlarged, subtriangular, not pointed posteriorly, connected posteriorly by a large, round scale; scales on ventral surface of neck, granular smooth, juxtaposed; scales on ventral surface of abdomen and chest smooth, cycloid; scales on femoral and precloacal region larger than those on the abdomen, smooth; 170–172 longitudinal scales from mental to cloaca, mid-body scales 29–32; distinct enlarged metacarpal scale present below digit I; subdigital lamellae under fourth digit of manus 18, under fourth digit of pes 19–21; males with 7–11 precloacal pores; 11 precloacal pores in BNHS 2921 holotype male, ten precloacal pores arranged in a single row, with an additional one positioned above in the attached row; femoral pores absent on each thigh; scales on dorsal surface of forelimbs un-keeled, imbricate, juxtaposed; dorsal scales of thigh and tibia weakly keeled, imbricate;

enlarged, keeled, conical tubercles at dorsal surface tail are more larger than those on dorsal body; dorsal scales on tail flattened, un-keeled, imbricate posteriorly, intermixed with enlarged, strongly keeled, pointed, conical enlarged tubercles; enlarged tubercles on the tail forming whorls, rest of the tail with decreased in size with paravertebral tubercles; median series of subcaudals slightly larger than rest, not widened; dorsal colour of head, neck and upper body brownish-yellow with distinct fresh-yellow bands; dorsal aspect of the body, bellow forelimbs and limbs are grey above with irregular white and black markings; dorsal aspect of tail grey with alternating 4 or 5 black and white bands.

Comparisons with members of *C. beddomei* clade.

Cnemaspis rashidi **sp. nov.** is a member of the *C. beddomei* clade and can be easily distinguished from all fourteen members of the clade by a combination of the following differing or non-overlapping characters: SVL less than 50 mm (vs. SVL<45 mm in *C. aaronbaueri* Sayyed *et al*. 2019, *C. azhagu* Khandekar *et al.* 2022, *C. galaxia* Pal *et al.* 2021, *C. nairi* Inger *et al*. 1984, *C. nigriventris* Pal *et al*. 2021, *C. regalis* Pal *et al.* 2021, *C. rubraoculus* Pal *et al.* 202, more than 55 mm in *C. anamudiensis* Cyriac *et al*. 2018); dorsal scales of body granular, intermixed with enlarged, fairly regularly arranged, strongly keeled, pointed, conical tubercles (vs. randomly arranged weakly keeled, large tubercles in *C. aar-onbaueri*, *C. beddomei* (Theobald, 1876), *C. maculicollis* Cyriac *et al.* 2018, partially keeled, rounded enlarge tubercles in *C. nairi* Inger *et al*. 1984, *C. regalis*, *C. rubraoculus*); 10–11 tubercles in paravertebral rows (vs. 8–10 in *C. aaronbaueri*, 2–3 in *C. azhagu*, 10–12 in *C. beddomei*, eight in *C. galaxia*, 16–18 in *C. nairi*; 13–14 in *C. nigriventris*, 12–14 in *C. nimbus* Pal *et al*. 2021, 7–9 in *C. regalis*, 8–10 in *C. rubraoculus*, 19–22 in *C. smaug* Pal *et al*. 2021 and 14–15 in *C. wallaceii* Pal *et al.* 2021); mental enlarged, subtriangular, not pointed posteriorly, connected posteriorly by a large, round scale (vs. mental subpentagonal, pointed, not connected posteriorly by median scale in *C. galaxia*, mental triangular in *C. nigriventris*; mental subpentagonal, connected posteriorly by median wide scale in *C. nimbus*; mental pointed, roughly triangular, not connected posteriorly by median scale in *C. regalis*; mental subpentagonal, connected posteriorly by median wide scale in *C. rubraoculus*; mental roughly conical, posteriorly in contact with two rounded scales in *C. wallaceii*); males with 7–11 precloacal pores (vs. 7–8 in *C. aaronbaueri*, 2–3 in *C. anamudiensis*, 6–8 in *C. azhagu*, 7 in *C. beddomei* and *C. galaxia*, 10 in *C. maculicollis*, 7–8 in *C. nairi*, 6–7 in *C. nigriventris*, 4–6 in *C. nimbus*, 6–8 in *C. regalis*, 6 in *C. rubraoculus*, 7–8 in *C. smaug* and 8 in *C. wallaceii*); 170–172 longitudinal ventral scales from mental to cloaca (vs. 135–140 in *C. aaronbaueri*, 154 in *C. beddomei*, 153–159 in *C. galaxia*, 154–159 in *C. nigriventris*, 143–147 in *C. nairi*, 134–141 in *C. nimbus*, 148–154 in *C. regalis*, 122–133 in *C. rubraoculus*, 142–150 in *C. Smaug* and 154–156 *C. wallaceii*); 29–32 ventral scales across belly at midbody (vs. 34–44 in *C. azhagu*, 30–34 in *C. beddomei*, 27–31 in *C. galaxia*, 38–40 in *C. nigriventris*, 26–27 in *C. nimbus*, 40–44 in *C. regalis*, 30–34 in *C. smaug* and 28–29 in *C. wallaceii*); lamellae under fourth digit of pes 19–21 (vs. 24–25 in *C. aaronbaueri* and *C. nigriventris*, 24–27 in *C. azhagu* and *C. regalis*, 23–25 in *C. galaxia*, 23–24 in *C. maculicollis*, 27–28 in *C. nairi*). *Cnemaspis rashidi* **sp. nov.** is morphologically close to *C. ornata* (Beddome, 1870), based on a combination of characteristics it can be easily distinguished from *C. ornata* by having SVL up to 50 mm (vs. 46.1 mm in *C. ornata*); 10–11 tubercles in paravertebral rows, 170–172 longitudinal scales from mental to cloaca, 29–32 midventral scales, males with 7–11 precloacal pores (vs. 16 paravertebral rows, 157–165 longitudinal scales from mental to cloaca, 33–37 midventral scales and 6–7 precloacal pores); lamellae under fourth digit of pes 19–21 (vs. 28–31); distinct enlarged metacarpal scale present below digit I (vs. no enlarged metacarpal scale below digit I in *C. ornata*). Dorsal colour of head grey with white stripes, six to seven white spots longitudinally along mid vertebral from nuchal region to base of the tail in *C. ornata* vs. dorsal colour of head brown with bright-yellow stripes, five lighter white spots longitudinally along mid vertebral from the forelimbs to base of the tail in *Cnemaspis rashidi* **sp. nov.**

Description of the holotype. An adult male generally in good state of preservation (Fig. 1 A, B). 47.50 mm SVL, head short (HL/SVL 0.29), not depressed (HD/HL 0.36), not wide (HW/HL 0.58), distinctly larger from neck. Loreal region slightly inflated, canthus rostralis not prominent. Snout less than half of head length (ES/HL 0.43); scales on snout and canthus rostralis large, round, juxtaposed, un-keeled, much larger than those on forehead and interorbital region; scales on occipital and temporal region small, round, un-keeled, granular (Fig. 2 A). Eye small (ED/HL 0.12), with round pupil; supraciliaries not elongate. Tympanum deep, ear-opening rounded, smaller than head length (EOD/HL 0.05); eye to ear distance longer than diameter of eye (ET/EOD 5.64), ear-opening approximately half of diameter of eye (EOD/ED 0.42). Rostral much wider (2.55 mm) than high (1.63 mm), divided dorsally, rostral groove present; enlarged supranasal on each side, twice in the size of postnasals, contacted with each other, internasal scale absent; rostral in contact with supralabial I, nasal and supranasal; nostrils small, oval, bordered by two postnasals, supranasal and rostral; three rows of small scales separate the orbit from the supralabials (Fig. 2 C). Mental enlarged, subtriangular, not pointed posteriorly, longer (3.11 mm) than wider (2.68 mm); two pairs of postmentals, inner pair large, connected with each other, separated by a large, round scale, posterior-postmentals small, postmentals bordered posteriorly by 12 smaller, rounded scales, middle three scales in row are larger than other; gular scales small, granular, juxtaposed, smooth; throat scales, small, flat, juxtaposed, same in size those on gular (Fig. 2 B). Supralabials up to angle of jaw eight on the right and eight left side; supralabial I larger than II in size, not decreasing in size posteriorly; infralabials up to angle of jaw seven on the right and seven on the left side; infralabial I and II equal in size. Canthal region with 16 scales on both sides; supraciliaries separated by 36 scales at midorbit. Body relatively short, trunk less than half of SVL (AG/SVL 0.37) without ventrolateral folds. Dorsal pholidosis heterogeneous; composed of circular granular scales intermixed with enlarged, fairly regularly arranged, strongly keeled, pointed, conical tubercles in 11 longitudinal rows, extending from limb insertion to tail

(Fig. 3 A, C); number of mid-dorsal scales 74; scales on flanks small, granular, smooth, larger conical and spine-like tubercles absent on either side of the lower flanks (Fig. 3 C). Granular scales on nape un-keeled, slightly smaller than those on paravertebral rows, scales on occiput un-keeled, similer in size than those on nape. Scales on ventral surface of neck, granular smooth, juxtaposed; scales on chest, smooth, cycloid; scales on ventral surface of abdomen between limb insertion smooth, cycloid; mid-ventral scales 170, mid-body scales 32 across the ventral between the lowest rows of dorsal scales (Fig. 3 D); scales on femoral and precloacal region larger than those on the abdomen; ten precloacal pores arranged in a single row, with an additional one positioned above in the attached row (Fig. 2 D). Forelimbs moderately long, slender; dorsal scales of brachium un-keeled, imbricate, juxtaposed; dorsal scales of forearm un-keeled, imbricate, slightly smaller than those on brachials; ventral scales of brachium granular, smooth, raised, smaller than those on forearm; scales beneath forearm, smooth, flat, cycloid; palmar scales smooth, slightly raised; claws slightly recurved; dorsal scales of thigh and tibia weakly keeled, imbricate; ventral scales of thigh and tibia flat, cycloid; subtibial scales weakly keeled; plantar scales smooth, raised; digits long with an inflected joint; subdigital lamellae notched; lamellae beneath first phalanges slightly widened (Fig 2 E, F); subdigital lamellae on finger I: 12, finger II: 14, finger III: 18, finger IV: 18, finger V: 15; toe I: 12, toe II: 15, toe III: 20, toe IV: 19 and toe V: 18. Relative length of digits, fingers: IV (4.32 mm)>V (4.06 mm) >III (4.04 mm)>II (3.69 mm) >I (3.15 mm); toes: IV (5.54 mm) >V (5.03 mm) >III (4.50 mm) >II (4.05 mm) >I (1.77 mm). Tail entire and original, cylindrical, moderately slender, flattened beneath, longer than snout-vent length (TL/SVL 1.24). Dorsal scales at tail base granular, similar in size and shape to those on mid-body dorsum, gradually becoming larger, flatter, un-keeled intermixed with enlarged, more larger than those on dorsal body, keeled, conical tubercles; dorsal scales on tail flattened, un-keeled, imbricate posteriorly, intermixed with enlarged, strongly keeled, pointed, conical enlarged tubercles; enlarged tubercles on the tail forming whorls, rest of the tail with decreased in size with paravertebral tubercles (Fig. 3 A, B). Scales on ventral aspect of tail larger than those on dorsal aspect, subimbricate, smooth; median series slightly larger than rest, not widened; scales on tail base slightly smaller than those on mid-body ventrals, smooth, imbricate; a single, conical, small postcloacal spur on each side.

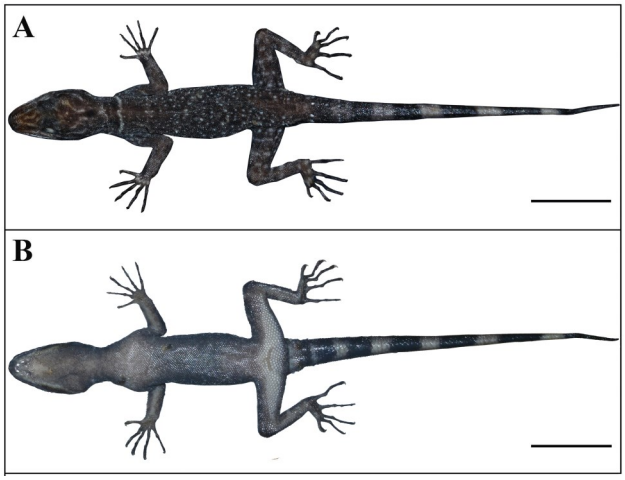

Figure 1. *Cnemaspis rashidi* **sp. nov.,** holotype, BNHS 2921; (A) dorsal view of body, (B) ventral view of body. Scale bars 10 mm. Photos by Amit Sayyed

Colouration of male in life (Fig. 4). The dorsal aspect of the lower body bellow forelimbs insertion is grey intermixed with distinct black and white small scattered, spots; dorsal colour of head to upper body dark-brown; bright-yellow and black small markings on forehead and snout, dorsal aspect of head more dark with bright-yellow bands and black marks; supraciliaries yellow with black spots; laterally a slender, bright-yellow postocular band continues occipital on both side separated by a black ocellus; a slender, bright-yellow band runs each side laterally from first supralabial continuing backwards covering the supralabials and extending through the ear, separated by a middle yellow spot; infralabials black; bright-yellow band dorsally between forelimb insertion; five lighter white spots longitudinally along mid vertebral from forelimbs to base of the tail; the limbs are grey above with irregular white and black markings; digits are grey with

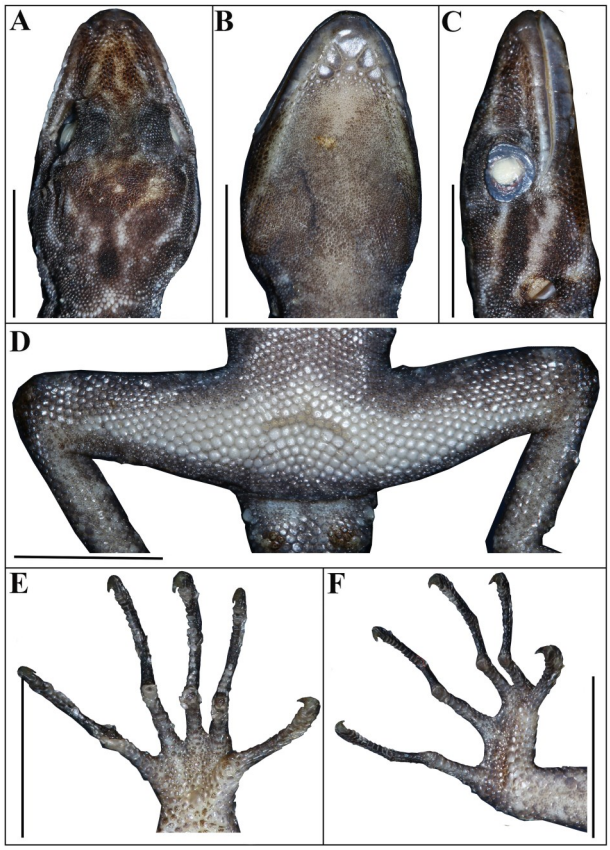

Figure 2. *Cnemaspis rashidi* **sp. nov.,** holotype, BNHS 2921; (A) dorsal view of head, (B) ventral view of head, (C) lateral view of head, (D) view of femoral and precloacal region, (E) ventral view of lamellae under right menus, and (F) ventral view of lamellae under right pes. Scale bars 5 mm. Photos by Amit Sayyed

irregularly alternative black and white spots. Dorsal aspect of tail grey with white and black bands, alternating 4 or 5 black and white bands. The ventral side of the head dirty-grey with irregularly yellow and brown spots, ventral side of body dirty-grey; ventral side of tail grey with dull- white with black bands.

Colouration of male in preservative (Fig. 1 A, B). Dorsum of the head and neck with yellow which turns into dark brown, fresh-yellow markings and bands on dorsal head, lateral head and neck which turns into dull-white, dorsum of the body and limbs with grey which turns into dark-brown, white markings and bands in life turns into dull- white in preservation; ventral side of head, body and tail grayish-white.

Colouration of female in life. The dorsal aspect of the head, body, limbs, and tail is brown, intermixed with dull-white markings. The dorsal color of the head is brown with small, dull-white spots on the forehead and snout. The dorsal aspect of the head exhibits three slender dull-white bands: the first is on the dorsal head, the second on the occiput, separated by a central black ocellus, and the third on the nape, separated by a central white spot. A dull-white band is present dorsally between the forelimb insertions, separated by a central white spot; seven lighter white spots longitudinally along mid vertebral from nape to base of the tail. The dorsal aspect of the tail is brown with alternating dull-white and black bands, with 4 or 5 bands in each sequence. On the ventral side, the body is grey, while the ventral side of the tail is grey with dull-white and black bands.

Colouration of female in preservative. Dorsum of the head, body, limbs and tail with brown which turns into grey, white markings and bands on dorsal head, body, limbs and tail which turns into light-grey in preservation; ventral side of head, body and tail white-grayish.

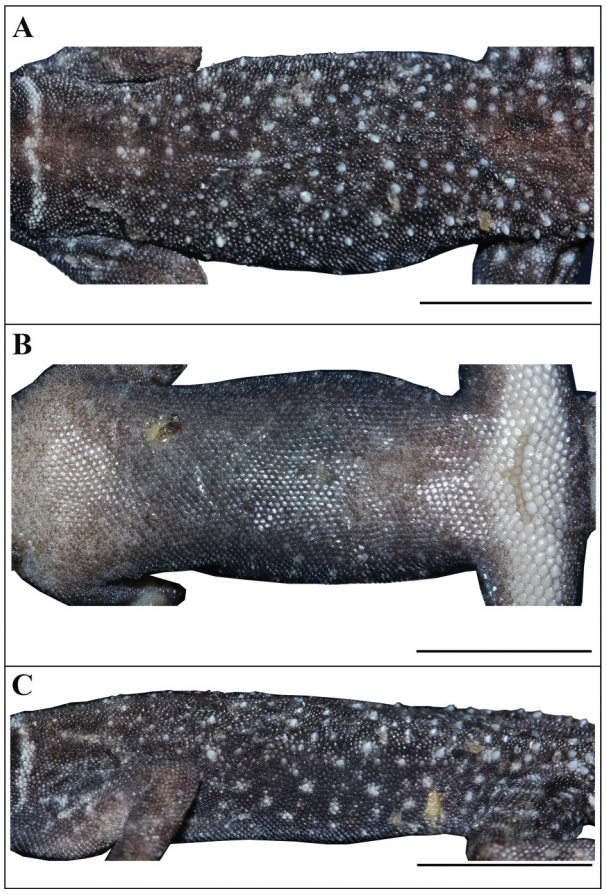

Figure 3. *Cnemaspis rashidi* **sp. nov.,** holotype, BNHS 2921; (A) dorsal view of mid-body, (B) ventral view of mid-body, and (C) lateral view of mid body. Scale bars 5 mm. Photos by Amit Sayyed

Figure 4. Colour in life of *Cnemaspis rashidi* **sp. nov.,** holotype, BNHS 2921 male. Photos by Amit Sayyed

Table 2. Mensural data for the type series of *Cnemaspis rashidi* **sp. nov.,** (Measurements are in mm).

Measurements	Holotype BNHS 2921	Paratype BNHS 2922	Paratype BNHS 2923	Paratype BNHS 2924
Sex	male	female	male	male
SVL	47.50	47.29	49.93	42.34
AG	17.75	18.77	18.99	15.84
TW	8.95	9.79	8.10	6.08
ED	1.75	1.59	1.69	1.23
EN	5.50	4.75	5.68	5.17
ES	6.11	5.63	6.51	5.87
ET	4.23	4.19	3.82	3.50
IN	1.13	1.14	1.11	1.10
EOD	0.75	0.74	0.78	0.71
HL	14.14	13.34	14.56	12.11
HW	8.34	8.26	9.12	7.47
HD	5.21	5.06	5.81	5.10
IO	4.73	5.02	4.87	4.02
UAL	8.36	9.06	9.19	7.90
FAL	8.10	8.14	8.74	7.10
FL1	3.15	2.82	3.23	2.45
FL2	3.69	3.63	3.95	3.41
FL3	4.04	4.25	4.16	3.97
FL4	4.32	4.39	4.39	4.21
FL5	4.06	3.69	4.24	3.77
FEL	9.15	8.90	9.03	8.26
TBL	10.76	10.24	10.63	9.02
TOL1	1.77	2.04	2.13	1.65
TOL2	4.05	4.86	4.12	3.57
TOL3	4.50	5.28	5.02	3.99
TOL4	5.54	5.56	6.15	4.96
TOL5	5.03	5.46	5.94	4.81
TL	59.37	50.88	55.81	50.33

Table 3. Morphometric and meristic data of the type series of *Cnemaspis rashidi* **sp. nov., (**– = data not present).

Character	Holotype BNHS 2921	Paratype BNHS 2922	Paratype BNHS 2923	Paratype BNHS 2924
Sex	male	female	male	male
SupL R/L	8/8	8/7	8/7	8/7
InfL R/L	7/7	7/7	7/7	7/7
SuS	23	22	23	23
InO	36	37	36	36
BeT	26	24	26	27
PoN	2	2	2	2
PoM	2	2	2	2
PoP	12	13	11	12
SuN	2	2	2	2
CaS	16	16	16	16
MbS	74	73	74	75
DtR	11	10	10	11
MvS	170	171	172	170
BIS	32	32	29	31
PPores	11	–	9	7
MLam R	12/14/18/18/15	12/15/20/18/15	11/15/18/18/16	12/13/18/18/15
PLam R	12/15/20/19/18	12/13/20/21/21	12/15/20/20/18	12/14/20/20/18

Variation. Mensural and meristic data for the type series are given in Table 2 and Table 3. There are four specimens (two an adult males, a female and a sub-adult male) ranging in SVL from 42.34 mm to 49.93 mm. All paratypes resemble the holotype except as follows: the number of supralabials ranges from seven to eight to the angle of jaw, 8 supralabials on left side in BNHS 2921 holotype male, 7 in all paratypes; the number of lamellae on digit I of the manus ranges from 11–12; the number of lamellae on digit IV of the pes from 19–21; scales surrounded by the posterior-postmentals and between infralabials ranges from 11–13; ventral scale counts in longitudinal and transverse series vary from 170–172 and 29–32, respectively; number of mid-dorsal scales ranges from 73–75; 7 precloacal pores present in sub-adult specimen BNHS 2924, 9 in BNHS 2923 and 11 precloacal pores in BNHS 2921 holotype male, ten precloacal pores arranged in a single row, with an additional one positioned above in the attached row. The three males in our collection match in overall colouration with each other, female do not match in colouration with males; there is strong sexual dichromatism in this species.

Natural History. (Fig. 5) The new species was found in the premises of a private property situated in the higher elevations of the southern Western Ghats. The individuals were found dwelling on the rock boulders and walls in the private property. The field observations suggest that the new species exhibits diurnal behaviour and is notably inactive during nigh-time. The individuals were exclusively observed at the higher elevations of the mountain range with no records at lower elevations. The new species was found to be sympatric with *Ophiophagus hannah* (Cantor, 1836), *Craspedocephalus malabaricus* (Jerdon, 1854), and *Lycodon travancoricus* (Beddome, 1870).

Distribution (Fig. 7). Currently, *Cnemaspis rashidi* **sp. nov.** is known only from its type locality from Kottamalai estate, Settur, Rajapalayam, Viridhunagar, Tamil Nadu, India

Discussion

The *C. beddomei* clade is restricted to the southern Western Ghats and diversified ~46 Mya during the Eocene to early Oligocene (Pal *et al.* 2020). The diversification was based on hill ranges and climatic regimes. *Cnemaspis ornata* Beddome, 1870 from the *C. beddomei* clade was described from South Tinnevelly Hills in Tamil Nadu, India. Manamendra-Arachchi *et al.* (2007) in their monograph designated lectotype and para-lectotypes of *C. ornata*. Furthermore, Pal *et al.* (2020) in their study identified *C. ornata* from Vairavankulam RF, Tirunelveli, Tamil Nadu, India and generated its sequences. Based on the ND2 sequence generated by Pal *et al.* (2020), *C. rashidi* **sp. nov.** shows a divergence of 9.5–9.7%. Moreover, after examining the specimen CESL 276 of *C. ornata* identified by Pal *et al.* (2020) it matches the description of the lectotype. Considering the morphology, *Cnemaspis rashidi* **sp. nov.** shows a significant divergence from the lectotype of *C. ornata*. The type locality of *C. rashidi* **sp. nov.** is ~41 km from the Vairavankulam RF, Tirunelveli, Tamil Nadu aerially. In support of these facts and previously observed micro-endemism within the genus (Sayyed *et al.* 2019; Agarwal *et al.* 2022; Narayan *et al.* 2023; Sayyed *et al.* 2023 a,b), *C. rashidi* **sp. nov.** being a new species cannot be denied. The new species descriptions persist

across various hill ranges in peninsular India. The description of *C. rashidi* **sp. nov.** indicates the micro-endemism within the genus and emphasises the need for further conservation efforts.

Figure 5. Habitat photo of *Cnemaspis rashidi* **sp. nov.** from Kottamalai estate, Settur, Rajapalayam, Viridhunagar, Tamil Nadu, India. Photos by Amit Sayyed

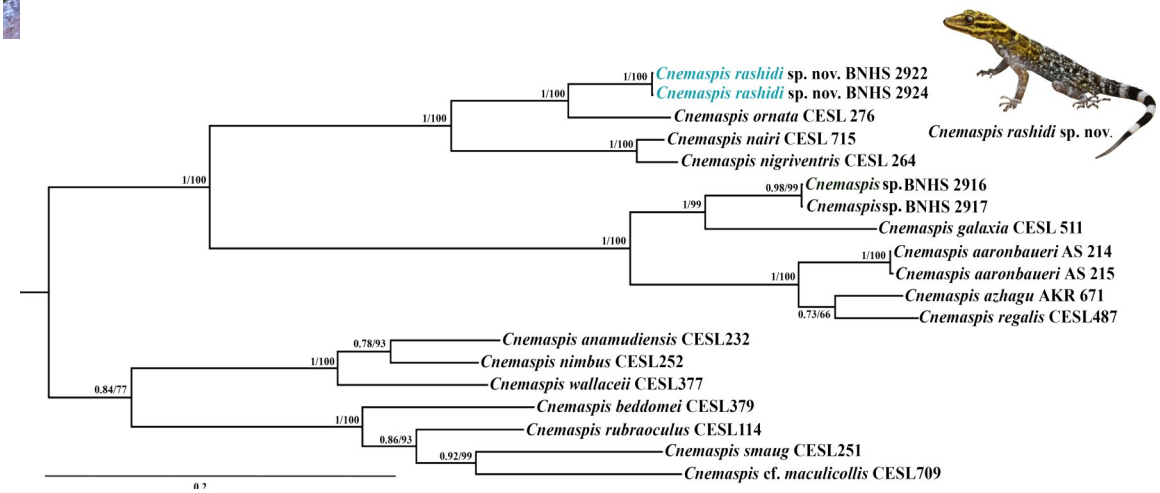

Figure 6. A cladogram showing the phylogenetic relationships of the species in the *Cnemaspis beddomei* clade (ND2+16S rRNA)

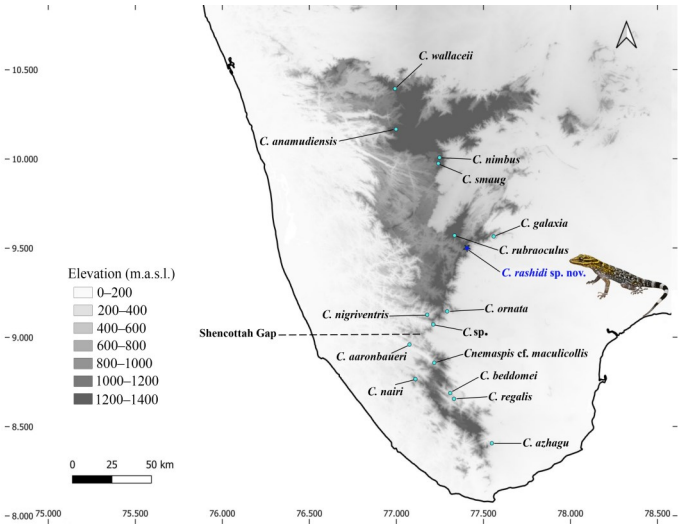

Figure 7. Map showing the distribution of *Cnemaspis beddomei* Theobald, 1876 clade in southern peninsular India. The type locality of the new species is indicated by a star.

ACKNOWLEDFEMENTS

The authors express their gratitude to the Forest Departments of Tamil Nadu for their invaluable support during field surveys. We would like to thank the Director of the Bombay Natural History Society, Mumbai, for generously facilitating access to specimens and overseeing the registration of the type specimens. Furthermore, the dedicated efforts of Kamesh Salunkhe and Aman Adsul from the Wildlife Protection and Research Society (WLPRS) are warmly acknowledged for their assistance. The authors are also thankful to the Wildlife Protection and Research Society (WLPRS) and Insearch Environmental Solutions (IES) for the laboratory facilities and institutional support.

REFERENCES

Agarwal, I., Thackeray, T., and Khandekar, A. 2022. A multitude of spots! Five new microendemic species of the *Cnemaspis gracilis* group (Squamata: Gekkonidae) from massifs in the Shevaroy landscape, Tamil Nadu, India. *Vertebrate Zoology*,

Biju, S.D., Garg, S., Gururaja, K.V., Shouche, Y., and Walujkar, S.A. 2014a. DNA barcoding reveals unprecedented diversity in Dancing Frogs of India (Micrixalidae, *Micrixalus*): a taxonomic revision with description of 14 new species. *Ceylon Journal of Science* (*Biological Sciences*), 43(1): 37−123.

Edgar, R.C. 2004. MUSCLE: multiple sequence alignment with high accuracy and high throughput. Nucleic Acids Research 32 (5): 1792– 1797.https://doi.org/10.1093/nar/gkh340

Kalyaanamoorthy, S., Minh, B.Q., and Wong T.K. F. 2017. ModelFinder: Fast model selection for accurate phylogenetic estimates. Nature Methods 14: 587–589

Kumar, S., Stecher, G., and Tamura, K. 2016. MEGA7: Molecular Evolutionary Genetics Analysis Version 7.0 for Bigger Datasets. Molecular biology and evolution 33: 1870– 1874.

Lanfear, R., Calcott, B., Ho, Y.W.S., and Guindon, S. 2012. PartitionFinder: Combined Selection of Partitioning Schemes and Substitution Models for Phylogenetic Analyses. Mol. Biol. Evol. 29 (6):1695–1701. doi:10.1093/molbev/mss020

Leary, S., Underwood, W., and Lilly, E. 2013. Guidelines for the Euthanasia of Animals. American Veterinary Medical Association.

Loria, S.F., and Prendini, L. 2020. Out of India, thrice: diversification of Asian forest scorpions reveals three colonizations of Southeast Asia. *Scientific Reports*. 10: 22301. https://doi.org/10.1038/s41598-020-78183-8.

Macey, J.R., Larson, A., and Ananjeva, N.B. 1997. Two novel gene orders and the role of light-strand replication in rearrangement of the vertebrate mitochondrial genome. Molecular Biology and Evolution 14: 91–104.

Manamendra-Arachchi, K., Batuwita, S., and Pethiyagoda, R. 2007. A taxonomic revision of the Sri Lankan day-geckos (Reptilia: Gekkonidae: *Cnemaspis*), with description of new species from Sri Lanka and southern India. *Zeylanica*, 7(1), 9-122.

Mani, M.S. 1974. Biogeography of peninsular India. Pp. 614–645. In Ecology and biogeography in India. (eds M.S. Mani), Dr. W. Junk Pulishers.

Minh, B. Q., Schmidt, H.A., Chernomor, O., Schrempf, D., Woodhams, M.D., Von Haeseler, A., Lanfear, R., and Teeling, E. 2020. IQ-TREE 2: New models and efficient methods for phylogenetic inference in the genomic era. Molecular Biology and Evolution 37(5): 1530–1534. https://doi.org/10.1093/molbev/msaa015

Narayanan, S., Pal, S., Grismer, L.L., and Aravind, N.A. 2023. A new species of rupicolous Cnemaspis Strauch, 1887 (Squamata: Gekkonidae) from the Male Mahadeshwara Wildlife Sanctuary, southern Eastern Ghats, India. Vertebrate Zoology, 73, 189-203.

Nguyen, L.T., Schmidt H.A., Von Haeseler A., and Minh, B.Q. 2015. IQ-TREE: A fast and effective stochastic algorithm for estimating maximum-likelihood phylogenies. Molecular Biology and Evolution 32: 268–274.

Pal, S., Mirza, Z.A., Dsouza, P., and Shanker, K. 2021. Diversifying on the Ark: Multiple new endemic lineages of dwarf geckos from the Western Ghats provide insights into the systematics and biogeography of South Asian *Cnemaspis*. *Zoological Research*, 42, 675−691. https://doi.org/10.24272/j.issn.2095-8137.2021.074.

Rambaut, A., Drummond, A.J., Xie, D., Baele, G., and Suchard, M.A. 2018. Posterior summarization in Bayesian phylogenetics using Tracer 1.7. Systematic Biology 67, 901 –904. https:// doi.org/10.1093/sysbio/syy032

Ronquist, F., Teslenko, M., Van Der Mark, P., Ayres, D.L., Darling, A., Höhna, S., Larget, B., Liu, L., Suchard, M.A., and Huelsenbeck, J.P. 2012. Mrbayes 3.2: Efficient bayesian phylogenetic inference and model choice across a large model space. Systematic Biology 61, 539–542. https://doi.org/10.1093/sysbio/sys029

Sayyed, A., Grismer, L.L., Campbell, P.D., and Dileepkumar, R. 2019. Description of a cryptic new species of *Cnemaspis* Strauch, 1887 (Squamata: Gekkonidae) from the Western Ghats of Kerala State of India. *Zootaxa*, 4656(3): 501-514

Sayyed, A., Kirubakaran, S., Khot, R., Abinesh, A., Harshan, S., Sayyed, A., Sayyed, M., Adhikari, O., Purkayastha, J., Deshpande, S., and Sulakhe, S. 2023a. A New Rupicolous Day Gecko Species (Squamata: Gekkonidae: *Cnemaspis*) from Tamil Nadu, South India. *Taprobanica*, 12(01), 5–13.

Sayyed, A., Kirubankaran, S., Khot, R., Harshan, S., Adhikari, O., Sayyed, A., Sayyed, M., Fazil, A., Jerith, A., Deshpande, S., Purkayastha, J., and Sulakhe, S. 2023b. Two new species of *Cnemaspis* Strauch, 1887 (Squamata: Gekkonidae) from southern India. *Zootaxa* (In press).

Schwarz, G. 1978. Estimating the Dimensions of a Model. The Annals of Statistics. Vol. 6, No, 2, 461– 464

Tamura, K., and Nei, M. 1993. Estimation of the number of nucleotide substitutions in the control region of mitochondrial DNA in humans and chimpanzees. Molecular Biology and Evolution 10 (3): 512–526. https://doi.org/10.1093/oxfordjournals.molbev.a040023

Uetz, P., Freed, P., Aguilar, R., Reyes, F., and Hošek, J. 2023. The Reptile Database, http://www.reptile- database.org, accessed [09 / 09/ 2023]

Vijayakumar, S.P., Menezes, R.C., Jayarajan, A., and Shanker, K. 2016. Glaciations, gradients, and geography: multiple drivers of diversification of bush frogs in the Western Ghats Escarpment. *Proc. R. Soc*. B 283: 20161011. https://doi.org/10.1098/rspb.2016.1011.

Appendix 1

No	Species	16S r RNA	ND2	Locality
1	*Cnemaspis aaronbaueri*	OR708521	OR714926	India, Kerala, Kollam, Thenmala
2	*Cnemaspis aaronbaueri*	OR708522	OR714927	India, Kerala, Kollam, Thenmala
3	*Cnemaspis anamudiensis*	MZ291574	MZ701805	India, Kerala, Idukki
4	*Cnemaspis azhagu*	-	ON494554	India, Tamil Nadu, Kalakad Mundanthurai Tiger Reserve,
5	*Cnemaspis beddomei*	MZ291581	MZ701814	India, Tamil Nadu, Kalakkad Mundanthurai TR,
6	*Cnemaspis galaxia*	MZ291589	MZ701818	India, Tamil Nadu, Virudhu-nagar, Srivilliputhur,
7	*Cnemaspis cf. maculioculis*	MZ291582	MZ701825	India, Kerala, Kollam, Shendur-ney Wls
8	*Cnemaspis nairi*	MZ291608	-	India, Kerala, near Shendurney, Thenmala
9	*Cnemaspis nigriventris*	MZ291609	MZ701808	India, Kerala, Achankovil RF
10	*Cnemaspis nimbus*	MZ291612	MZ701807	India, Kerala, Idukki, Mathiket-tan Shola NP
11	*Cnemaspis ornata*	MZ291613	MZ701809	India, Tamil Na-du,Tirunelveli,Vairavankulam RF
12	*Cnemaspis rashidi sp. nov.*	-	OR714921	India, Tamil Nadu, Virudhu-nagar, Settur, Rajapalayam, Kottamalai estate.
13	*Cnemaspis rashidi sp. nov.*	-	OR714922	India, Tamil Nadu, Virudhu-nagar, Settur, Rajapalayam, Kottamalai estate.
14	*Cnemaspis regalis*	MZ291615	MZ701816	India, Kalakkad Mundanthurai TR, Tamil Nadu
15	*Cnemaspis rubraoculus*	MZ291616	-	India, Kerala, Upper Manalar, Periyar Tiger Reserve,
16	*Cnemaspis smaug*	MZ291618	MZ701806	India, Kerala, Idukki, Mathiket-tan Shola NP
17	*Cnemaspis sp.*	-	OR714924	India, Tamil Nadu, Tenkasi, Shenkottai, Mekkarai, Into the wild Resort
18	*Cnemaspis sp.*	-	OR714925	India, Tamil Nadu, Tenkasi, Shenkottai, Mekkarai, Into the wild Resort
19	*Cnemaspis wallaceii*	MZ291619	MZ701813	India, Tamil Nadu, Anamalai, Andiparai Shola

Appendix 1. List of GenBank accession numbers of ND2 and 16S r RNA sequences used in the analyses. Newly generated sequences in this study were deposited in the GenBank® nucleotide sequence database and are written in bold in the table.